





Article

Relevance and Reliability of Outdoor SO₂ Monitoring in Low-Income Countries Using Low-Cost Sensors

Rosa Amalia González Rivero ¹, Olivier Schalm ², Arianna Alvarez Cruz ¹, Erik Hernández Rodríguez ³, Mayra C. Morales Pérez ¹, Daniellys Alejo Sánchez ^{1,*}, Alain Martínez Laguardia ³, Werner Jacobs ² and Luis Hernández Santana ³

¹ Faculty of Chemistry, Universidad Central “Marta Abreu” de Las Villas, Road to Camajuaní Km 5.5, Santa Clara 54830, Villa Clara, Cuba

² Antwerp Maritime Academy, Noordkasteel Oost 6, 2030 Antwerpen, Belgium

³ Faculty of Electrical Engineering, Universidad Central “Marta Abreu” de Las Villas, Road to Camajuaní Km 5.5, Santa Clara 54830, Villa Clara, Cuba

* Correspondence: daniellysas@uclv.edu.cu

Abstract: In the Western world, the SO₂ concentration in ambient air dropped to low levels, but some emission sources (e.g., merchant ships) and some regions (e.g., low-income countries) still emit substantial amounts of SO₂. At those locations, SO₂ monitoring is critical. However, low-income countries do not have much access to expensive reference instruments. Low-cost gas sensors might be an alternative, but it is unclear how reliable such measurements are. To evaluate the performance of the low-cost alternative, the same SO₂ gas sensor has been subjected to three different calibration methods: (1) low-cost calibration performed in the tropical climate of Cuba; (2) high-end calibration performed in Belgium; (3) a field calibration at an air quality measuring station in Belgium. The first two methods showed similar trends, suggesting that the gas sensor can be calibrated with a low-cost method. The field calibration was hampered by the low SO₂ concentrations. For the monitoring campaign in Cienfuegos, Cuba, the low-cost SO₂ sensor calibrated by the low-cost method appeared to be sufficiently reliable. The reliability of the sensor increases with the increase in SO₂ concentration, so it can be used in Cuba instead of Belgium.

Keywords: pollutants; SO₂; low-cost sensors; low-cost calibration; reliability; Cuba



Citation: González Rivero, R.A.; Schalm, O.; Alvarez Cruz, A.; Hernández Rodríguez, E.; Morales Pérez, M.C.; Alejo Sánchez, D.; Martínez Laguardia, A.; Jacobs, W.; Hernández Santana, L. Relevance and Reliability of Outdoor SO₂ Monitoring in Low-Income Countries Using Low-Cost Sensors. *Atmosphere* **2023**, *14*, 912. <https://doi.org/10.3390/atmos14060912>

Academic Editor: László Benics

Received: 2 March 2023

Revised: 15 May 2023

Accepted: 19 May 2023

Published: 23 May 2023



Copyright: © 2023 by the authors. Licensee MDPI, Basel, Switzerland. This article is an open access article distributed under the terms and conditions of the Creative Commons Attribution (CC BY) license (<https://creativecommons.org/licenses/by/4.0/>).

1. Introduction

Belgium was the first country in continental Europe to follow the UK into the industrial revolution. Heavy industries such as iron foundries or glass production settled in the proximity of rivers and coal mines in the south of Belgium during the 19th century. However, this economic success also had a downside [1–4]. Air pollution and acidifying deposition were suspected to damage vegetation (e.g., oaks, fruit trees, crops) and cause nuisance by the mid-19th century. However, the relationship between air pollution and mortality was only confirmed after the deadly fog in the Meuse Valley on 1–5 December 1930 [5,6]. During the Meuse Valley incident, hundreds of people endured pulmonary attacks, and 63 people suddenly died in Engis, Belgium. This disaster triggered multiple scientific studies and led to the first scientific proof that pollution could cause deaths and diseases. The source of harm appeared to be the combustion of coal. Since fossil fuels such as coal or crude oil contain 1–2% sulphur by weight, they emit smoke and SO₂ when burned. People exposed to the fog inhaled sulphuric acid. Similar disasters occurred at other locations, with the most famous being the Great Smog in London on 5–9 December 1952 [7–10]. At that time, the average SO₂ concentration in London was around 70 ppb, with a peak at 1339 ppb on December 8 [11]. Since then, legislation, abatement strategies, and emission control measures have been implemented [12]. After 1970, global SO₂ emission started to drop in Europe [13]. In Europe and North America, the SO₂ concentrations

became so low that acid rain, which caused, among other things, accelerated dissolution of limestone in historical statues and monuments [14], is not a major issue anymore. Today, ambient SO₂ concentrations in Belgium are in the range of 1–2 ppb, with some peaks up to 20 ppb [15,16]. These concentrations are close to the detection limit of low-cost SO₂ gas sensors, and it is unclear if such sensors collect reliable data in such regions. With ‘reliable,’ we mean some useful information can be extracted from sensor readings to evaluate air quality while operating in a real-world application.

Nevertheless, SO₂ emissions are still significant in certain sectors, such as merchant shipping, where heavy fuel containing sulphur (<0.5%) is used as fuel outside the SECA areas (i.e., regions at sea where sulphur content in fuel must be lower than 0.1%). SO₂ emissions also occur in rapidly growing regions such as East and South Asia. This is also a problem in low-income countries, where the urgency to remove sulphur from crude oil is lower than other issues. For example, Cuba produces mainly heavy crude oil, which contains 7 to 8% sulphur by weight [17–19]. This feature leads to increased SO₂ emissions during combustion. In addition, Cuban oil exhibits several distinct features, including a high asphaltene content, a low API gravity (i.e., American Petroleum Institute gravity), and elevated concentrations of heavy metals such as nickel and vanadium. These metals are known to contribute to the generation of particulate matter (PM) during combustion. According to data from the Central Bank of Cuba, fuel oil production in 2020 was around 3.8 million tons, which represented 41% of the national demand [20]. The rest of the demand was imported from Venezuela, Russia, or Algeria. In addition to these countries, Cuba has also imported fuel oil from other countries such as Mexico, Angola, Brazil, China, and Nigeria, although to a lesser extent. The derivatives, such as diesel oil or fuel oil, have higher fossil-fuel emission factors for SO₂ than the desulfurized equivalents used in the Western world. In addition, the use of old technologies in industry and transportation leads to higher fuel consumption levels. At the same time, the treatment of atmospheric emissions is insufficient. Despite the fact that Cuba’s economic situation makes it impossible to replace existing technologies with more efficient and less polluting alternatives in the short term, there is a need to control SO₂. Because of the large number of diesel engines that act as SO₂ sources, there is a particular need for low-cost control systems.

Recently conducted net emission inventories in Cuba showed that the following pollutants can be ranked in decreasing importance: SO₂ > NO₂ > CO [21]. This suggests the importance of SO₂ as a pollutant in Cuba. A Gaussian dispersion modeling system for pollutants suggests that the maximum concentration of SO₂ in rural environments is 30 ppb [22]. Another study performed in Santa Clara City, Cuba reported an average concentration of 4 ppb for the period February to April 2010 [23]. In Havana, a study about air pollution due to vehicular traffic revealed SO₂ average concentrations between 5 and 15 ppb, with peaks of up to 60 ppb [24]. These studies suggest that the average SO₂ concentration in the air is higher in Cuba than in Belgium.

It is known that the reliability of low-cost sensors is lower in comparison with high-end and expensive trace-level UV fluorescence analysers that are considered the gold standard [25–29]. Therefore, one must know the most important calibration problems (e.g., no access to high-end equipment to perform calibrations, the effect of a tropical climate, etc.), the impact of varying environmental parameters, and the interference of other pollutants on the measurements to ensure the best possible reliability of the collected data [30,31]. This contribution will explore the reliability of low-cost SO₂ monitoring. It will be illustrated with a measuring campaign performed in Antwerp, Belgium, on the roof of an air quality monitoring station analysing outdoor air, and a measuring campaign performed in Cienfuegos, Cuba.

2. Background

Electrochemical 4-electrode gas sensors are widely used in air quality monitoring and toxic gas detection applications due to their relative high sensitivity and selectivity [32–35]. A well-known example of such low-cost gas sensors are the ones of the manufacturer

Alphasense. They are provided with calibration information. However, the accurate calculation of pollutant concentrations remains a challenge [36,37]. According to the manufacturer, the sensors register the voltages corresponding to the working electrode (WE) and auxiliary electrode (AE). The WE provides information about the target analyte, while the AE is designed to mimic the WE in the absence of the target gas while considering the response to changes in meteorological conditions such as temperature and relative humidity. Despite the apparent simplicity of the formulas to calculate the concentration from WE and AE, the information about Alphasense is confusing. This leads to different interpretations of the formulas in the literature. Some assume a correction factor n_T equal to 1 [38–40]. Others consider n_T a constant provided in tabular or in graphic form by Alphasense [41,42]. For the Alphasense SO₂-A4 sensor, the manufacturer suggests for n_T a value of 0.4 in one document [43] and 1.15 in another document [44]. It is not clear whether these variations are due to a change in the construction of the electrochemical cell. In the 2014 Alphasense Application Note AAN 803-01, “Correcting for background currents in four electrode toxic gas sensors”, n_T is defined as the ratio WE_0/AE_0 for zero air at the temperature at which the measurement is performed. This definition suggests a variable ratio. The scientific literature has demonstrated that corrections of WE and AE recommended by the manufacturer do not always lead to pollutant concentration values with acceptable precision [45]. There are several factors that can affect the accuracy of gas concentration measurements, such as cross-sensitivity, drift, calibration, and other environmental factors that can interfere with the sensor signal.

The voltage values of both electrodes for air without pollutants (WE_0 and AE_0) can be obtained from a calibration process using zero air. The ratio allows the conversion of the measured AE-value into the corresponding background baseline $WE_{background}$. The background baseline that needs to be subtracted from WE can be calculated with Equation (1). If one assumes n_T as a variable ratio and the measured WE as the sum of the background baseline (i.e., $WE_{background}$) and a contribution that is concentration-dependent (i.e., WE_{gas}), then the formula of Alphasense can be obtained (see Equations (1)–(3)). Consequently, the sensor signal (WE_{gas}), expressed in mV, is directly proportional to the gas concentration.

$$n_T = \frac{WE_0}{AE_0} = \frac{WE_{background}}{AE} \Leftrightarrow WE_{background} = \frac{WE_0}{AE_0} AE, \quad (1)$$

$$WE = WE_{background} + WE_{gas} \Leftrightarrow WE_{gas} = WE - \frac{WE_0}{AE_0} AE, \quad (2)$$

$$WE_{gas} = WE - \frac{WE_0}{AE_0} AE + [n_T AE_0 - WE_0] = (WE - WE_0) - n_T (AE - AE_0). \quad (3)$$

Once the concentration-dependent signal WE_{gas} is calculated, the gas pollutant concentration expressed in ppb is calculated using Equation (4). The gas sensitivity (S_{gas}) is specific to each sensor, and its value is provided by the manufacturer. This means that the calculation of the concentration is a two-step process: (1) correct for the background baseline $WE_{background}$; (2) convert WE_{gas} into the corresponding concentration.

$$c_{gas} = \frac{WE_{gas}}{S_{gas}}. \quad (4)$$

It is usually assumed that n_T of the calibration process is identical to n_T of the measuring campaign. However, the contexts of both measurements are not necessarily the same, and this assumption may lead to an incorrect estimation of the background baseline $WE_{background}$. If there is no in situ zero air calibration available, then WE_0 and AE_0 can be estimated from the collected WE and AE time series. The moment t_{min} is characterized by the lowest WE-value in the time series, which is denoted by $WE_{min}(t = t_{min})$. The corresponding AE-value is given by $AE(t = t_{min})$. That moment is characterized by the minimum concentration, C_{min} . If the calibration curve is known, then C_{min} can be used

to calculate the corresponding $WE_{gas}(t_{min})$. There is often sufficient knowledge available about the measuring location to estimate C_{min} . For example, there will be a moment in the measuring campaign of SO_2 in outdoor air in Belgium when it will reach zero concentration. When AE_0 is not recorded at the same moment as WE_0 , the average of AE_0 in the time series can, in principle, be used to calculate the sensor signal.

We know that:

$$WE_{gas}(t_{min}) = WE_{min}(t_{min}) - WE_{background}(t_{min}) \quad (5)$$

therefore,

$$WE_{background}(t_{min}) = WE_{min}(t_{min}) - WE_{gas}(t_{min}) \quad (6)$$

$WE_{gas}(t_{min})$ can be expressed by the following formula if we clear it in Equation (4).

$$WE_{gas}(t_{min}) = S_{gas}C_{min}(t_{min}) \quad (7)$$

When $WE_{gas}(t_{min})$ is substituted into Equation (6), the following expression is obtained:

$$WE_{background}(t_{min}) = WE_{min}(t_{min}) - S_{gas}C_{min}(t_{min}) \quad (8)$$

In addition, we know that:

$$WE_{background}(t_{min}) = n_T AE(t_{min}) \quad (9)$$

therefore,

$$n_T = \frac{WE_{background}(t_{min})}{AE(t_{min})} \quad (10)$$

$WE_{background}$ in Equation (10) can be substituted by Equation (9) (see Equation (11)). When $C_{min} = 0$, Equation (11) can be further simplified, showing that n_T is the ratio WE_0/AE_0 for zero air.

$$n_T = \frac{WE_{min}(t_{min}) - S_{gas}C_{min}(t_{min})}{AE(t_{min})} \quad (11)$$

3. Materials and Methods

3.1. Low-Cost Monitoring System

The principles of low-cost monitoring systems have already been described in previous work [46,47]. Here, only the principle of the gas sensor measurements will be given in more detail. The SO_2 sensor type A belongs to one of the gas sensor families from the manufacturer Alphasense. It is inserted in an analog conditioning board (analog front end), designed by Alphasense to accommodate 4 different sensors (part number 810-0023-00). The configuration used includes sensors for NO_2 , OX ($O_3 + NO_2$), CO, and SO_2 . The analog front end (AFE) has an internal power supply of 3.3 V and only requires an input voltage between 3.5 and 6.5 V (DC). The conditioning board provides 8 analog outputs (2 for each sensor; more precisely, the “working electrode” and the “auxiliary electrode”) that must be wired to analog-to-digital converters (ADC). The sensitivity of the SO_2 sensor is 0.295 mV/ppb. The low-cost monitoring system that was used in the experiments consisted of an Arduino MEGA2560 as the computer unit and interface board, a real-time clock, and an SD card for data storage. The Arduino Mega 2560 contains an ADC with a 10-bit resolution. This ADC, with a reference voltage of 5 V, is capable of detecting voltage variations of about 4 mV. This means that it cannot detect changes of 1 ppb. To resolve this quantization problem, a pair of 4-channel analog-to-digital converters with 16-bit resolution (ADS 1115) have been added to the system. This resolution allows the detection of voltage changes of 0.076 mV, which is sufficient to detect 1 ppb concentration variations. The ADC has 4 analog inputs, hence the need to use 2 converters. The ADS 1115 module is connected to the Arduino Mega through the I2C communication protocol.

3.2. Sensor Calibration

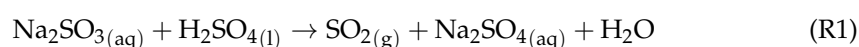
The calibration curve describes the relationship between the sensor signal and the reference measurements. Since that relationship must transform the sensor measurements into concentrations, the sensor signal is considered the independent variable. The same set of A-series Alphasense gas sensors for NO₂, O₃ (i.e., OX sensor), CO, and SO₂ has been subjected to 3 different types of calibration experiments. The experiments are summarized in Table 1 and include the most common calibration methods listed in the literature [48–52]. This work only focuses on the calibration of the SO₂ sensor. Calibration method 1 is a low-cost calibration method performed in Cuba using low-cost electronics purchased via the internet, medical disposables, and common laboratory equipment (e.g., balance, pipettes). This calibration method can be performed with a limited budget in low- or mid-income countries. The calibration setup needed is described elsewhere [53]. In the high-end calibration process number 2, all sensors have been exposed to the 4 different gases during separate calibration experiments. This makes it possible to evaluate the impact of NO₂, O₃, and CO gases on the signal of the SO₂ sensor, that is the cross-interference. This calibration method allows the sensor response to be compared with a reference analyzer. Sensor calibration methods under laboratory conditions are relatively fast. The concentration range of the pollutant and the temperature and relative humidity conditions can also be selected to perform the calibration. However, in these methods, the sensor is not exposed to real-field conditions. An advantage of field calibration is that data provided by low-cost sensors can be compared with official data reported by monitoring stations. This method is considered the most efficient because it allows the correction of meteorological and other pollutant fluctuations in the field environment by complex mathematical models. However, it is applicable only to the site where the calibration was performed. Another advantage of calibration method number 3 is that n_T for the outdoor calibration in ambient conditions must be fairly similar to the measuring location at a different outdoor location in the vicinity. The Alphasense formula with local values for WE₀ and AE₀ was used as well. A comparison of the different calibration processes makes it possible to evaluate the reliability of the low-cost calibration. Table 1 and the list below describe calibration experiments in detail.

Table 1. Overview of the calibration experiments performed on the same set of gas sensors, the period in which that calibration was performed, the average temperature, and relative humidity (RH) during the calibration process.

Nr.	Calibration Method	Location	T and RH Range	Calibration Period
1	Low-cost calibration of the SO ₂ sensor by generating SO ₂ gas inside a syringe	Santa Clara, Cuba	Tropical climate (23–25 °C and 62–65% RH)	19 November 2021
2	High-end calibration in a climate chamber using NO ₂ , O ₃ , CO and SO ₂ calibration gases	Mol, Belgium	Moderate marine climate (23 °C and 47–50% RH)	16–19 May 2022
3	Field calibration where the low-cost monitoring device is installed on the roof of the national outdoor air quality measuring station 42R802. The station is close to a crossroad.	Antwerp, Belgium	Moderate marine climate (10–30 °C, 30–94% RH)	30 May 2022–30 June 2022

- **Low-cost calibration in laboratory conditions:** The low-cost calibration setup consists of a closed plastic box that contains the gas sensor. The air inside the calibration box is first cleaned by pumping the air through a solution saturated with Ca(OH)₂. The cleaned air can be used to determine WE₀ and AE₀. First, SO₂ gas is generated inside a syringe. The gas is generated in a separate setup using the stoichiometric reaction R1 [54–56]. Graduated syringes with scale intervals of 0.2 mL were used.

One syringe contains 0.2 mL of 2.14 mol/L Na₂SO₃ solution. The second syringe contains 0.2 mL of concentrated 95% (*w/w*) H₂SO₄. The reagents are brought together to generate 9 mL of SO₂ gas in a third syringe. The acid solutions did not deteriorate the plastic setup and could be used for several calibration experiments. The amount of SO₂ inside the syringe expressed in moles can be calculated from its volume, the pressure of the gas inside the syringe, and the ambient temperature using the ideal gas law. Then, the syringe filled with SO₂ gas is connected to the calibration box using a pressure connection tube. One experiment entails several injections of small but known volumes of SO₂. The corresponding amounts of SO₂ introduced in the zero air inside the box were 110, 220, 330, 440, and 550 ppb. Each step lasted approximately 1 min. The low-cost calibration is performed by determining the relationship between the concentration-dependent sensor signal WE_{gas} and the reference SO₂ concentration injected into the plastic box.



- High-end calibration using a high-end climate chamber:** The set of NO₂, OX (i.e., the sum of O₃ and NO₂), CO, and SO₂ sensors is subjected to a calibration experiment at VITO, Belgium, which uses certified and traceable calibration gases to ensure the accuracy and reliability of the measurements. More detailed information on the calibration setup can be found elsewhere [53]. The temperature in the laboratory was controlled and kept at around 21 °C. The entire set of gas sensors was exposed to concentration ranges of 0 to 662.71 ppb, 0 to 145 ppb, 0 to 100 ppb, and 0 to 6 ppm of SO₂, NO₂, O₃, and CO, respectively, in separate calibration experiments. The gas sensors have also been submitted to the calibration experiment of the AM2315 sensor for temperature and relative humidity in the ranges of 20 to 50 °C and 5 to 80% RH. The calibration of the SO₂ sensor was performed in 1 experiment with continuous injections of the reference gas. A staircase profile with 12 SO₂ concentration levels was used. The reference concentrations were 27.44; 97.82; 239.18; 389.02; 532.92; 662.71; 540.00; 402.55; 257.70; 115.62; 43.10 and 4.51 ppb. Each step lasted between 3 and 4 h.
- Field calibration:** The sensor's performance was also evaluated by a field calibration, where the data provided by the low-cost sensor is compared to a reference measuring station that recorded reliable SO₂ concentrations. The calibration is conducted at station 42R801 of the Flemish Environment Society (Vlaamse Milieu Maatschappij VMM). The station generated a time series with a sampling time of 1 h. The low-cost monitoring systems used a sampling time of 2 min. With the function VLookUp in Microsoft Excel, the sensor data could be resampled so that values are obtained at the same timestamps as the measurements in the reference time series. The resampling allowed the integration of the two-time series into a single database. In this way, the relationship between the SO₂ sensor signal and the reference SO₂ concentration could be determined. Some authors consider that the duration of the field calibration is intrinsically related to the calibration model [57]. An optimal field calibration should cover all environmental conditions; therefore, it should be performed during different seasons and use complex mathematical models. In this study, the results obtained will be compared with calibration methods under laboratory conditions. For this reason, the simplest model (a linear regression model) and a shorter period during the summer were used. This season has the highest similarity to the Cuban climate. The field calibration in Antwerp, Belgium lasted 1 month. The visualization of the data recorded during the field calibration was generated with software developed by [58] in Python 3.

From the measured WE and AE data of the SO₂ gas sensor, the impact of how the concentration-dependent signal (WE_{gas}) is calculated on the calibration results will be discussed. This analysis was performed on calibration methods 1 and 2 from Table 1. The curves were compared with the Alphasense calibration. Alphasense calibration refers to the calculation of gas concentrations using Equations (3) and (4). A simple method is to

calculate the difference between the two electrodes (WE–AE). The sensor signal was also calculated by subtracting WE_0 from WE and using Equations (3) and (12). Equation (12) is similar to Equation (3), but the parameter n_T is not considered.

$$WE_{\text{gas}} = (WE - WE_0) - (AE - AE_0) \quad (12)$$

3.3. Reliability Testing

The reliability of an electrochemical gas sensor can be assessed through a number of indicators. Several reliability indicators are defined in the list below. They give an insight into the occurrence of calibration or measuring errors. By analyzing these indicators, an insight into the reliability of the measured concentration during the field campaign in Cienfuegos is obtained.

- The coefficient of determination of the linear regression between the sensor signal and the reference concentration is high, suggesting the absence of random errors during the calibration experiment.
- The stability of the SO_2 concentration inside the calibration box should be sufficiently long to perform a stable measurement of the signal at a given concentration.
- There is an agreement between the different types of calibration processes performed on the same sensor.
- The monitoring campaign can be considered reliable when the AE-signal remains constant over time or only gently fluctuates around its average;
- It is possible to remove the background baseline from the measured WE signal and obtain WE_{gas} .
- The detection and quantification limits of the gas sensor are sufficiently low so that the target gas is able to generate a reliable signal.
- The scientific literature gives evidence of the effect of cross-sensitivity in electrochemical sensors [59,60]. The sensor is reliable when the concentration of interfering gases is lower than the signal generated by the target gas or when a correction can be applied.
- Drift in the calibration constants of low-cost sensors can be caused by several factors, such as environmental conditions, lifetime, chemical decomposition, contamination, electromagnetic interference, and others. Measurements will be reliable when the drift in the calibration constants within the period of the calibration experiment and measuring campaign is sufficiently low. Sufficiently low means that the error introduced by drift is not significantly higher than other sources of error.
- The scientific literature demonstrates the influence of temperature and relative humidity on electrochemical sensor measurements [61,62]. Measurements will be sufficiently reliable when the interference of these variables on the measurement of the target gas is sufficiently low (i.e., the error is not significantly higher than other sources of error).

3.4. Measuring Campaign

A measuring campaign has been performed in Cienfuegos, Cuba, from 14 March to 22 April 2022, with a sampling time of 2 min. The urban historic centre of Cienfuegos is a part of UNESCO World Heritage, but Cienfuegos Bay is also an important harbour and industrial centre. The measuring location is situated 9 km south of the city ($22^{\circ}03'55''$ N, $80^{\circ}28'58''$ W), more specifically between the Caribbean Sea and Cienfuegos Bay (see Figure 1). The monitoring system has been placed outside at the Centro de Estudios Ambientales (CEAC) close to a window at a height of 2 m above ground level, according to the prescriptions of the Cuban standard NC 111:2014 [63]. The most important stationary pollution sources in the vicinity are the emissions from the Carlos Manuel de Céspedes thermoelectric plant, which uses national crude or fuel oil, and the Camilo Cienfuegos oil refinery. Examples of pollution sources closer to the measuring location are a small diesel power unit and a diesel combustion boiler. In addition, close to the sampling area, wood is burned for charcoal production. Figure 1 shows the location of the low-cost monitoring system and the most important pollution sources in its vicinity. The measuring campaign

resulted in a data matrix with measurements arranged in 27,852 rows and 9 parameters arranged in columns. The data matrix contains a column for the WE-value of the SO₂ sensor and another column for the corresponding AE-value. The visualization of the data recorded during the measuring campaign was also generated with the visualization software for environmental data.

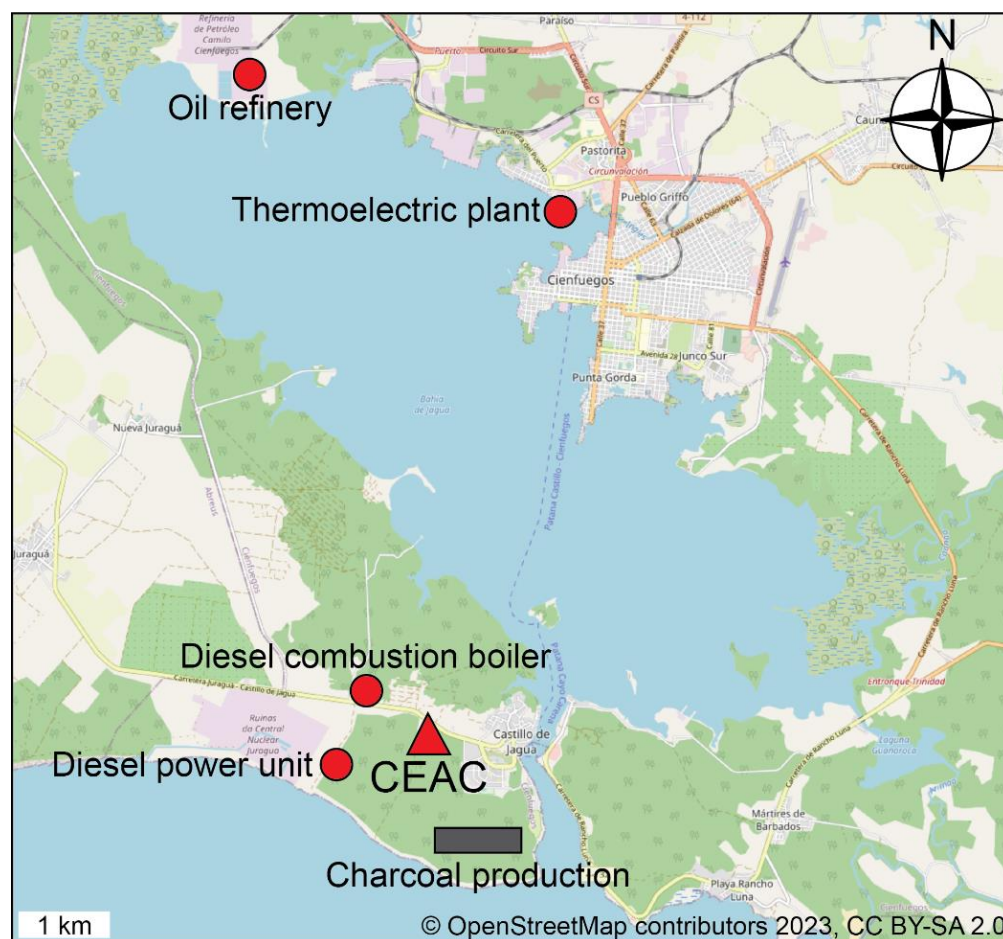


Figure 1. Map showing the sampling location in Cienfuegos, Cuba and the most important pollution sources in its vicinity.

4. Results

4.1. Sensor Calibration

The behaviour of the same SO₂ sensor subjected to different calibration experiments is shown in Figure 2. Each experiment generates raw signals for the WE and AE electrodes. This information is shown in Figure 2a,c,e. From the sensor data, the average concentration dependent signal, WE_{gas} must be calculated. The calculated signal is shown in the X-axes of Figure 2b,d,f where the relationships with the reference concentrations are described by linear regressions. The calibrations performed in laboratory conditions (Figure 2b,d) use elevated SO₂ concentrations and result in linear trends with high coefficients of determination (>0.99). These coefficients of determination can be used as reliability indicators. For the field calibration performed in Belgium, the SO₂ concentration range is smaller, and a fraction of that range falls below the detection limit of the low-cost sensor. The smallest detectable concentration must result in a signal that is higher than the random fluctuations around the average value of WE_0 , $\langle WE_0 \rangle + 3s_{WE_0}$, where $\langle WE_0 \rangle$ stands for the average signal at zero concentration and s_{WE_0} for the corresponding standard deviation. The minimum signal can be determined from point 12 in Figure 2c and compared with the signal at point 1, which appears to be just above the detection limit (i.e., 6.19 ppb). This

means that the data from almost the entire measuring campaign are below the detection limit of the sensor. It explains why the linear trend in the field calibration is not reliable. Besides these general observations, several specific conclusions can be drawn from the calibration experiments. They are described below.

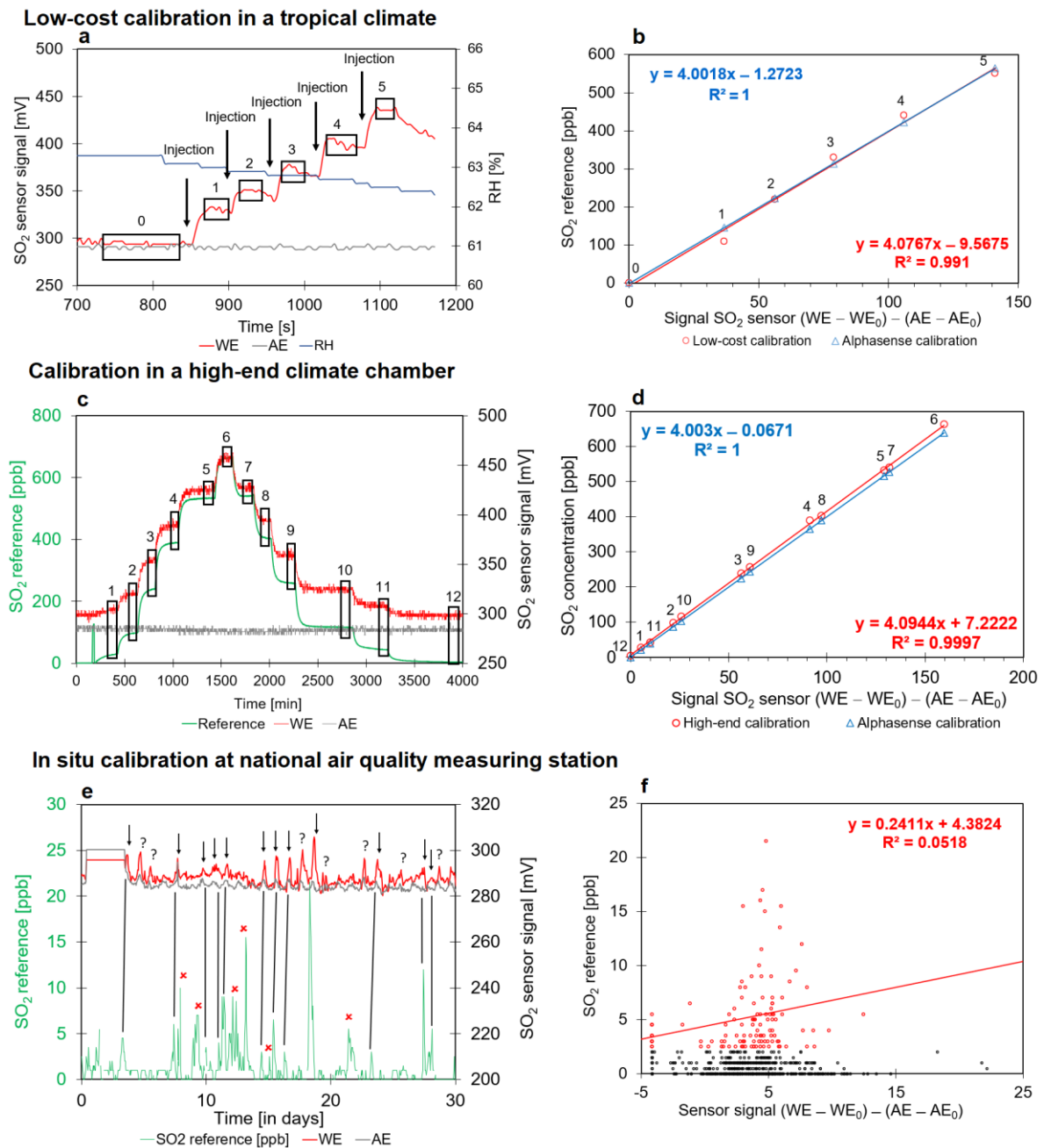


Figure 2. Different calibration processes applied on the same SO₂ sensor; the sensitivity is expressed in ppb/mV and the intercept in ppb. **(a,b)** Low-cost calibration under controlled conditions in laboratory performed in a tropical climate in Cuba. **(c,d)** High-end calibration under controlled conditions in laboratory performed in a moderate marine climate in Belgium. **(e,f)** Field calibration at a VMM air quality monitoring station, where the environmental conditions fluctuate in an uncontrolled way.

- **Low-cost calibration in laboratory:** The WE_0 and AE_0 signals of the SO_2 gas sensor in zero air (i.e., point 0 in Figure 2a) are 294.6 mV and 290.8 mV, respectively, with $n_T = 1.01$. The sensor measures the sudden jumps in the SO_2 concentration when the gas is injected in steps into the calibration box. The average values of the numbered rectangles in Figure 2a are used for calibration. A linear trend between sensor signal and SO_2 concentration is observed (Figure 2b). When using the sensor characteristics determined in zero air, the quantification method of Alphasense gives similar results to the low-cost calibration. The slopes for both methods are similar. However, there is a difference between the intercepts.
- **High-end calibration in laboratory:** The WE_0 and AE_0 signals of the same SO_2 sensor as used in the low-cost calibration in the laboratory in zero air (i.e., point 12 in Figure 2c) are 298.6 mV and 284.2 mV, with $n_T = 1.05$. This means that WE_0 and AE_0 are different from the ones at the low-cost calibration. The moments in Figure 2c marked with black rectangles indicate the stable measurements for each point in the calibration process. These moments are located in the second half of the plateaus because the chamber and sensor need some time to reach equilibrium. Figure 2d shows the linear trend between the average sensor signal from the numbered plateaus and the corresponding reference SO_2 concentration. In addition, Figure 2d also shows the calibration with the Alphasense formula (Equations (3) and (4)) using the characteristics determined at zero air in point 12. Both calibrations show a similar slope but a different intercept.
- **Field calibration:** To determine the local WE_0 and AE_0 , the minimum value for WE in the time series has been identified, together with the accompanying AE or average AE value (see Equation (5)). The reference concentrations clearly show that C_{min} within the time series reached zero. This gives 279 mV for WE_0 and 285 mV for AE_0 , which corresponds to $n_T = 0.979$. Each calibration experiment appears to be characterized by different WE_0 and AE_0 values. This suggests the need for in situ characterization of the sensor properties. During the measuring campaign, the reference monitoring system registered an average concentration of 0.5 ppb, with peaks of up to 20 ppb. In addition, 87% of the measurements are in the range of 0–2 ppb. Some of the peaks observed in the VMM data are also detected by the gas sensor with some time delay. At the same time, the gas sensor also shows SO_2 peaks that are not detected by VMM, and the VMM data contains peaks that are not detected by the gas sensor. Some peaks may be attributed to a cross-sensitivity effect and not to a significant SO_2 signal because, during the monitoring period, the concentrations of interfering gases such as NO_2 , O_3 , and CO were higher than that of SO_2 . This indicates that at locations with low SO_2 concentrations (e.g., Belgium), the low-cost sensor is not a good alternative for monitoring the pollutant concentration.

Figure 3 shows the different methods used to calculate the sensor signal. Although the calibration method of the manufacturer approached the low-cost calibration of Figure 2b and the high-end calibration of Figure 2d, a difference between both linear trends can be seen in Figure 3a when $WE-AE$ is used as a sensor signal. This difference is not caused by calibration errors but rather by an imperfect subtraction of the background baseline in the sensor signal. This error becomes smaller when the signals are processed differently (see Figure 3b–d). In addition, the experimental values of n_T in calibration methods 1, 2, and 3 are close to 1. For this reason and for the sake of simplicity, n_T is considered 1. Thus, Equation (12) was used to calculate the sensor signal and make the calibration curves shown in Figure 2. When local WE_0 and AE_0 values are used and the background contribution is determined as accurately as possible, both calibration processes result in similar calibration curves. It also means that the low-cost calibration performed on another continent can be considered sufficiently good to calibrate the gas sensor.

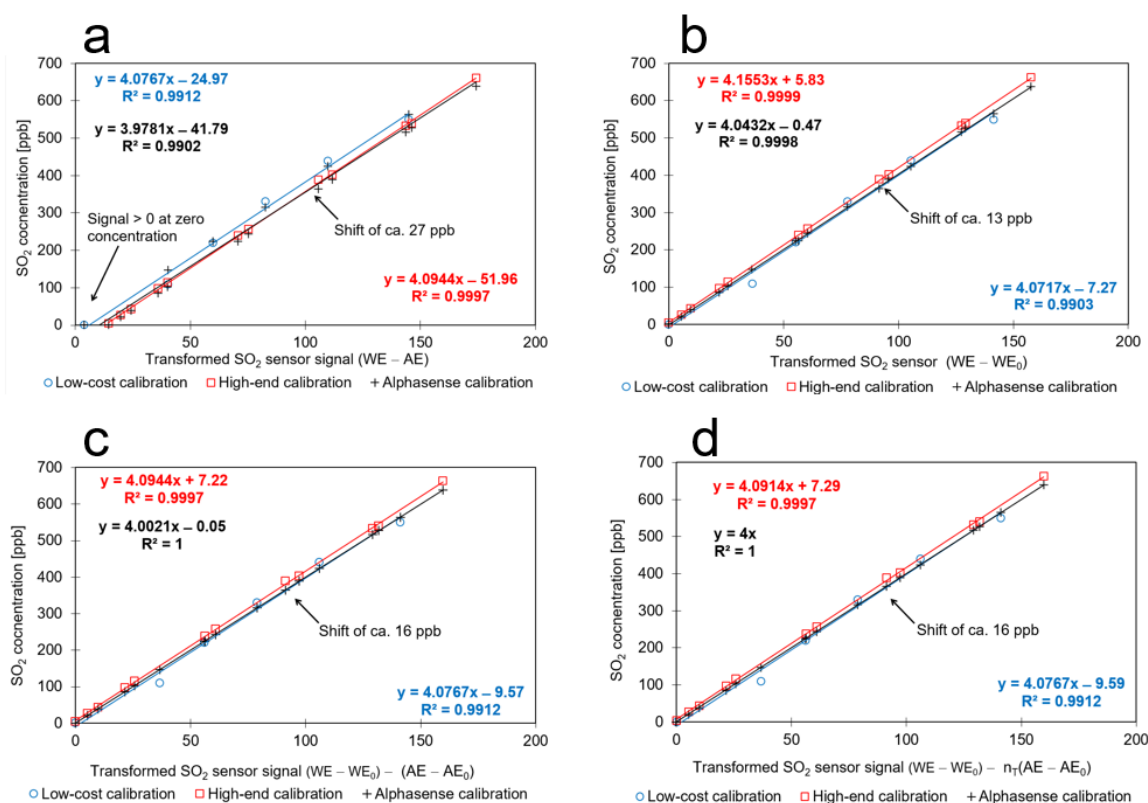


Figure 3. The calibration process of Figure 2a,c, where the concentration-dependent sensor signal has been calculated in different ways in comparison with the Alphasense equation using the appropriate WE₀ and AE₀ for both calibration processes. (a) The sensor signal has been calculated using the corresponding voltage values of both electrodes WE-AE; (b) The sensor signal has been calculated using the voltage values of the working electrode and the recorded value for zero air; (c) The sensor signal has been calculated using the voltage values of the working and auxiliary electrodes and the values recorded for zero air without considering n_T ; (d) The sensor signal has been calculated using Equation (3) suggested by the manufacturer.

Figure 2 shows that the low-cost calibration is sufficiently reliable under controlled conditions. However, it is unclear if the performance of the sensor is as good in real-life situations. For that reason, several aspects have been studied that give insight into the reliability of SO₂ measurements:

- **Coefficient of determination of the linear regressions:** The low-cost sensor showed a strong linear relationship with the reference concentrations in the calibrations performed under laboratory conditions (0.9912 and 0.9997 for the low-cost and high-end calibrations, respectively). This is an indication that the sensor can be considered reliable. However, the sensor was not reliable in the field calibration, obtaining a coefficient of determination of 0.0518.
- **Agreement between calibration processes:** The calibration curves shown in Figure 2 indicate that the low-cost calibration resulted in similar results as the high-end calibration. The high-end calibration resulted in concentrations that are systematically higher (ca. 17 ppb). However, the slopes are similar. Although the match of both calibration curves is not perfect, this observation gives satisfactory reliability to the low-cost calibration.
- **Stability of the SO₂ concentration inside the calibration box:** The sensor signal did not remain constant in the calibration box. The decreasing trend is most probably not caused by the air exchange rate because it occurs too fast. This behaviour might be attributed to a chemical reaction between SO₂ gas and water vapour. The resulting H₂SO₄ seems to remain invisible to the SO₂ gas sensor so, the concentration drops.

In addition, the RH in the box drops over time and seems to confirm our hypothesis (see Figure 2a). For each step in the low-cost calibration, the zones with the highest concentrations have been used as the most reliable situations.

- **Stability of the signal generated by the AE:** Although the AE signals of the three calibration experiments are different from each other, they appeared to be rather constant during the experiment. However, the AE signal during the field study contained peaks superposed on a slowly decreasing trend. It is not clear if this decreasing trend should be associated with a calibration drift because the background contribution can effectively evolve towards smaller values. It is unclear if this drop is caused by changing values for WE_0 and AE_0 . Figure 4a shows the trends of the auxiliary electrode of the SO_2 sensor when the NO_2 (red line), CO (blue line), and O_3 (green line) sensors were exposed to the high-end calibration. This behaviour is shown as a function of relative time in days. The AE trends of the SO_2 sensor show some fluctuations (see Figure 4a). During the NO_2 calibration, a decreasing AE trend for the SO_2 sensor is observed. The AE signal of the SO_2 sensor contains the staircase function of the CO concentration profile, while during the O_3 calibration, the AE signal of the SO_2 sensor appears to be rather constant. Apparently, there is a disturbance of the AE-signal of the SO_2 sensor when exposed to NO_2 and CO.
- **Possibility to remove the background level from the WE signal:** It is of primary importance that $WE_{background}$ can be estimated as accurately as possible. The baseline drift is mainly due to the variation in ambient environmental conditions. For this reason, the values of WE_0 and AE_0 as used for the calibration processes are not valid for the field campaign and need to be determined for the local situation. Once this is done, the calibration performed in laboratory conditions (span calibration) appears to be usable in the field campaign. This enhances the reliability of field campaigns using low-cost gas sensors.
- **Detection and quantification limits:** The lowest concentration that the SO_2 gas sensor can distinguish from zero air is the quantity that generates a signal that is at least equal to the average value of WE_0 , $\langle WE_0 \rangle$, plus 3 times the standard deviation of the signal fluctuating around $\langle WE_0 \rangle$ (i.e., limit of detection). The quantification limit is defined as $\langle WE_0 \rangle$ plus 10 times the standard deviation of the signal fluctuating around $\langle WE_0 \rangle$ [64]. This threshold can be determined with the data associated with point 12 in Figure 2c. The detection and quantification limits are 6.19 and 20.63 ppb, respectively. For measuring locations where the average SO_2 concentration is above the detection and quantification limits, the reliability of the measurements is sufficiently high. This was not the case during the field calibration in Belgium.
- **Cross-interference:** The concentrations of atmospheric pollutants CO, NO_2 , and O_3 are high in Cuba. Research about the quantification of tropospheric ozone in Cuba showed that in the cold season (from February to April), the concentration of this pollutant is high [65] and exceeds the threshold of 12 ppb as established by the Cuban standard NC 39:1999 [66]. The NO_2 quantifications showed that in the cold season the concentrations are higher, although not exceeding the admissible limit according to the Cuban standard [23]. This suggests that cross-interference can be expected and is probably more important than in Belgium because the interfering gases have higher concentrations than the target gas. During the high-end calibration of low-cost O_3 , NO_2 , and CO sensors, the SO_2 sensor signal was recorded when exposed to the other gases. This signal has been plotted as a function of the reference concentration of the pollutants (Figure 4b). The experiments show a linear response of the SO_2 sensor towards interfering gases. The SO_2 sensor has a negative linear response to O_3 and NO_2 , which corresponds to the information provided by Alphasense. It also corresponds with previous research [67,68]. Some report a negative response for CO [61], while this study shows a faint but positive correlation, which is in accordance with the information supplied by the manufacturer. It is likely that the responses vary from sensor to sensor. Thus, large CO-peaks might result in false SO_2 peaks,

while NO₂ and O₃ peaks should result in SO₂ valleys. Assuming the cross sensitivities are independent, the effects of the interfering gases on the SO₂ sensor signal can be corrected by the equations shown in Figure 4b. These results demonstrate the importance of using multi-sensor systems when low-cost sensors are used, as they provide the possibility of obtaining a better estimate of the cross-sensitivity.

- **Drift of the calibration constants:** The behaviour of the sensor during field calibration reflects a common trend with fluctuations (see Figure 2e). The trend might indicate that there is some drift. Since the monitoring campaign only took 1 month, this might be too short to observe obvious drifts. However, this suggests the need for periodic calibrations to assure reliability.
- **Interference of temperature and relative humidity:** As mentioned before, the SO₂ sensor was also subjected to the calibration experiment of the AM2315 sensor (T and RH). During these conditions, the SO₂ concentration was not measured with a reference instrument; however, in Belgium, the concentration fluctuates around 1 ppb (below the detection limit of the sensor). Moreover, the indoor SO₂ concentration is usually lower than the corresponding outdoor concentration. Therefore, any variation in the SO₂ sensor signal must be caused by the changing T and RH conditions in the climate chamber. The behaviour of the AM2315 sensor during the temperature calibration (Figure 4c) and the relative humidity calibration (Figure 4d) has been plotted as a function of time. The secondary axis of both graphs shows how the WE and AE signals of the SO₂ sensor respond to these conditions. Figure 4c shows that in the range of 20 to 30 °C, the sensor signals remain stable. With decreasing relative humidity from 80% down to 40% for a temperature of 20–30 °C, both WE and AE remained stable. At higher temperatures (i.e., 50 °C), the WE signal suddenly increases while AE decreases. In the range from 40% down to 5% at a temperature of 50 °C, the WE sensor signal shows a sudden increase that might be confused with a gas-specific signal. At this moment, the AE decreases but becomes stable afterwards. After exposure to 50 °C, the WE and AE are less stable in comparison to the range from 20 to 30 °C. This means that the sensor signal appears to have remained constant when the changing conditions remained in a relative cold (<30 °C) and humid (>40%) state. However, in warmer (>30 °C) but dryer (<40%) conditions, the sensor becomes very sensitive to small changes in the environmental conditions: the lower the RH, the higher the WE signal. This suggests that the sensor shows similar behaviour in moderate and tropical climates most of the time.

Figure 5 shows the gas and particulate matter concentrations recorded by the VMM station and the signal from the working and auxiliary electrodes of the low-cost SO₂ sensor during the field calibration in Antwerp, Belgium. The highest peaks recorded by the sensor are shown in this figure. The signal generated by the auxiliary electrode shows instability over time. Its trend is related to temperature peaks and relative humidity valleys. On some occasions, the high reference concentrations of SO₂ do not coincide with the sensor peaks (see more detail in Figure 2e). This is probably due to the low detection limit of the sensor. At other moments, when the peaks of the SO₂ reference are not recorded, sensor peaks are observed. These sensor peaks are related to temperature peaks and relative humidity valleys but also to peaks of O₃ (see the red rectangles in Figure 5). Although the NO₂ concentration is higher than the SO₂, no strong relationship between the recorded peaks was observed. Only one peak of CO is simultaneously related to the peaks of NO₂ and SO₂ (see the black rectangle in Figure 5). At that moment, the VMM station also recorded a small peak of SO₂. The simultaneous peaks suggest that the pollutants are generated by the same pollution sources [68]. The occurrence of simultaneous peaks for different pollutants and the SO₂ peak caused by interference is sometimes hard to distinguish.

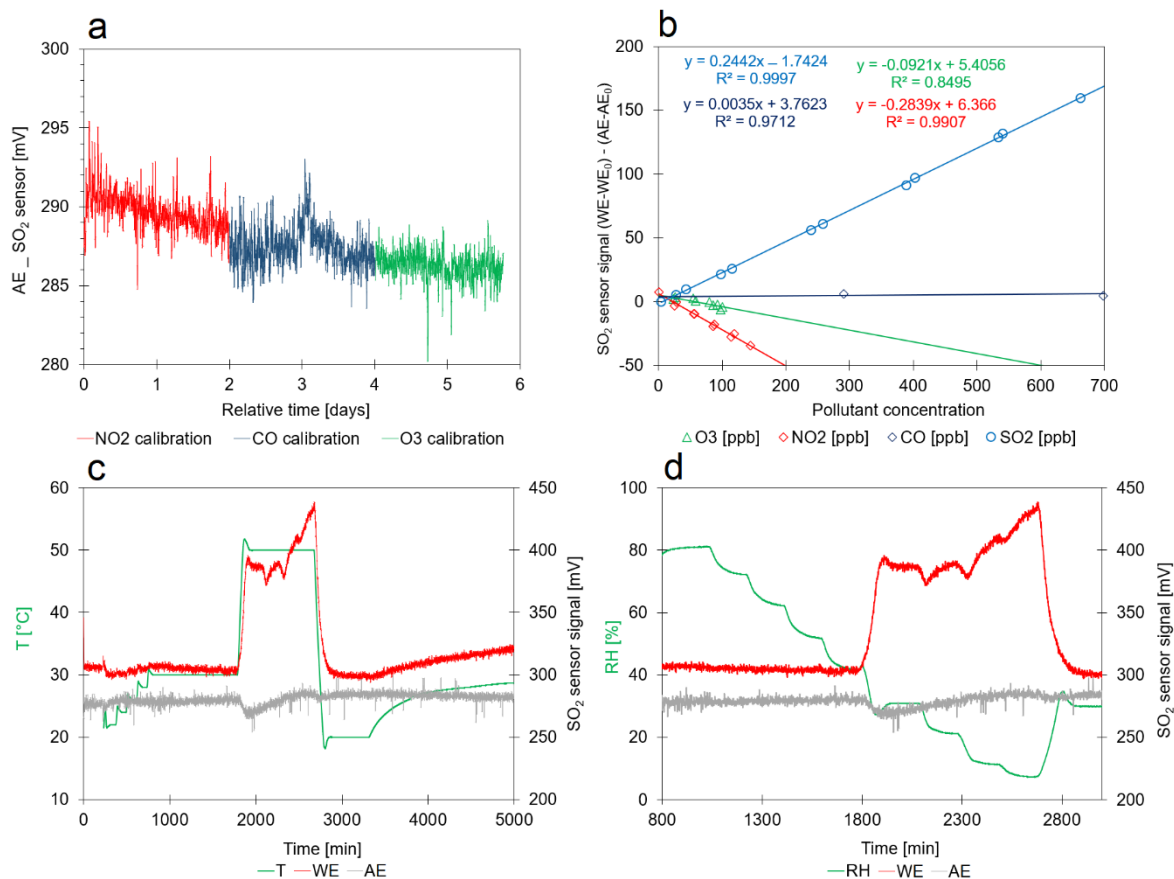


Figure 4. Impact of different pollutants and environmental conditions on the low-cost SO₂ sensor signal. (a) AE SO₂ sensor signal trends during the high-end calibration with NO₂, CO, and O₃; (b) cross-interference effect on the SO₂ sensor signal; (c) sensor signal trends at different temperature levels while the RH is changed in steps; (d) sensor signal trends at different relative humidity levels while the temperature changes are shown in (c).

4.2. Measuring Campaign in Cienfuegos, Cuba

When analyzing the AE values over time, this parameter shows fluctuations around an average of 284.2 mV. The minimum value for WE is 282 mV, with a corresponding AE value of 276 mV, resulting in an n_T of 1.02. The analysis of WE₀ and AE₀ during the calibration processes and the measuring campaign in Cuba also show that these values cannot be considered sensor constants because different values were obtained in all cases. Therefore, they have to be determined for every measuring campaign. As can be seen in Table 2, they change from campaign to campaign. To understand these fluctuations, it is necessary to perform more in-depth studies over a longer period of time. Some authors suggest that they are due to changes in environmental conditions such as temperature, relative humidity, pressure, and trace contaminants [69]. However, when n_T is calculated, values close to 1 are obtained in all cases.

Table 2. Overview of WE₀ and AE₀ from the different measuring campaigns. The campaigns are ranked chronologically.

	Low-Cost Calibration	High-End Calibration	Field Calibration	Measuring Campaign in Cuba
WE ₀	294.6	298.6	279.0	282.0
AE ₀	290.8	284.2	285.0	276.0
n_T	1.01	1.05	0.979	1.02

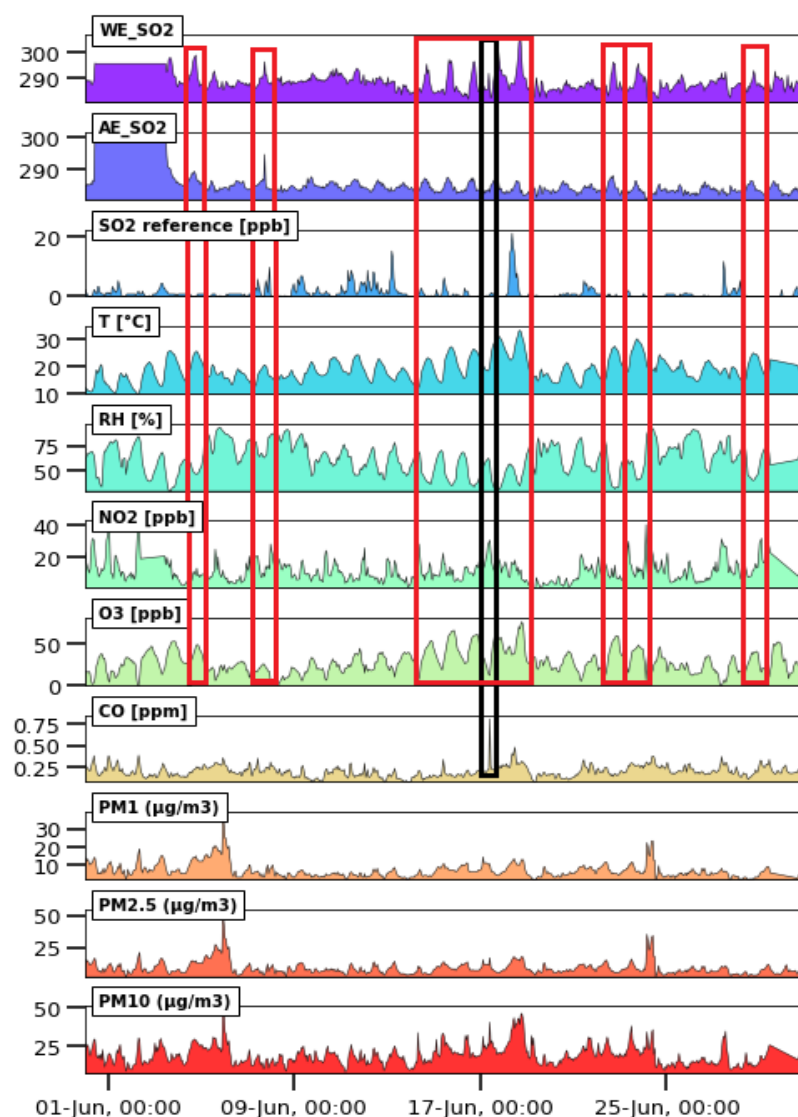


Figure 5. Concentration of gases and particulate matter recorded by the VMM station and the signal of the working and auxiliary electrodes of the low-cost SO₂ sensor during the field calibration performed in Antwerp, Belgium, from 30 May to 30 June 2022. The red rectangles indicate the simultaneous relationship of the SO₂ sensor with some parameters recorded by the station such as temperature, relative humidity, SO₂, NO₂ and O₃. The black rectangle indicates the simultaneous relationship of the SO₂ sensor with NO₂ and CO.

In the measuring campaign at Cienfuegos, the WE signal is clearly larger than the AE value. Figure 6a shows that the AE signal develops a slowly decreasing trend with superposed peaks. The minimum value for AE does not correspond with the minimum value for WE. The values for WE₀ and AE₀ are determined as the minimum value from the WE time series and the average value of the AE time series. The average value is used instead of the corresponding AE value of WE_{min}, as suggested by Equation (11), but both values are similar. In addition, the concentration-dependent signal WE_{gas} is significantly larger than zero, suggesting that the SO₂ concentration at the measuring location is above the detection limit of the sensor. When applying the low-cost and high-end calibrations, the same trend is observed (Figure 6b). The main difference is that the high-end calibration results in a shift of about 17 ppb. Despite this shift, it seems that the two calibration curves can be used for quantification if the background baseline of WE is removed in both the calibration processes and the field study. The monitoring campaign falls within the temperature range of 20–30 °C and the relative humidity range of 40–80%, so these

variables do not affect the reliability of the SO₂ measurements. Figure 6 shows two periods in which the SO₂ concentration decreases appreciably. This behaviour can be related to the variation of the wind direction, which changed from east, east northeast to north, north northeast. These conditions favored the transport and dispersion of the pollutant to occur further away and in a different direction from the sampling site. In both periods, precipitation also occurred, which led to the removal of SO₂ [70]. The limited amount of information about the average SO₂ concentration in Cienfuegos, Cuba can be enriched with the average concentration as determined from the trends. Depending on the low-cost or high-end calibration, the average concentration ranges from 31.62 ppb to 48.59 ppb. These values are above the detection and quantification limits of the sensor. Therefore, the SO₂ sensor measurements recorded during the field campaign in Cienfuegos, Cuba show higher reliability than the measurements recorded in Belgium. The reliability can be further improved when the concentration range of the calibration process matches that of the measuring campaigns. The low-cost calibration process used 110 ppb as the lowest concentration.

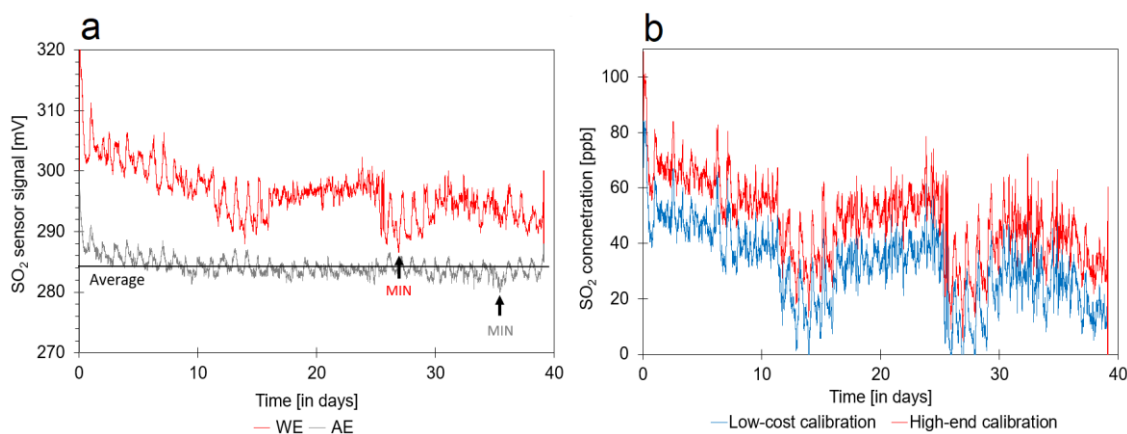


Figure 6. Measuring campaign performed in Cienfuegos. (a) Trends of WE and AE electrodes over time. (b) SO₂ concentrations have been calculated with the low-cost and high-end calibration process.

For this measuring campaign, the trends of the other gas sensors have been shown as well (see Figure 7). For this analysis, the NO₂, O₃, CO, and SO₂ concentrations were determined by using the equation obtained from the high-end calibration. It is important to mention that the O₃ signal was determined by subtracting the NO₂ signal from the O_x signal. Figure 6 shows some simultaneously occurring peaks of CO, PM, and SO₂ (see the black rectangles in Figure 7). The peaks can be related to: (1) the pollution source because the burning of, for example, diesel results in the simultaneous emission of SO₂, CO, PM, non-methane volatile organic compounds (NMVOCs), and other pollutants [71,72]; or (2) a cross-sensitivity effect due to the CO concentration in the air that is higher than that of SO₂. On the other hand, valleys in the SO₂ trend are observed when NO₂ or O₃ show peaks (see the red rectangles in Figure 7). The impact of NO₂ on the SO₂ signal is less notable since the NO₂ concentration is not considerably higher than that of SO₂. This might be explained by chemical reactions where SO₂ is being transformed into sulfates [73] or by a cross-sensitivity effect of the sensor. In addition, SO₂ peaks are observed that are not correlated with other pollutants, such as an increase in the SO₂ concentration at the sampling site or an increase in an interfering compound that is not measured (e.g., VOCs, H₂S, etc.). More background information is needed to understand how reliable the observed peaks are, but the correlation between peaks suggests the burning of diesel as a pollution source. This would have been missed if only average concentrations had been available.

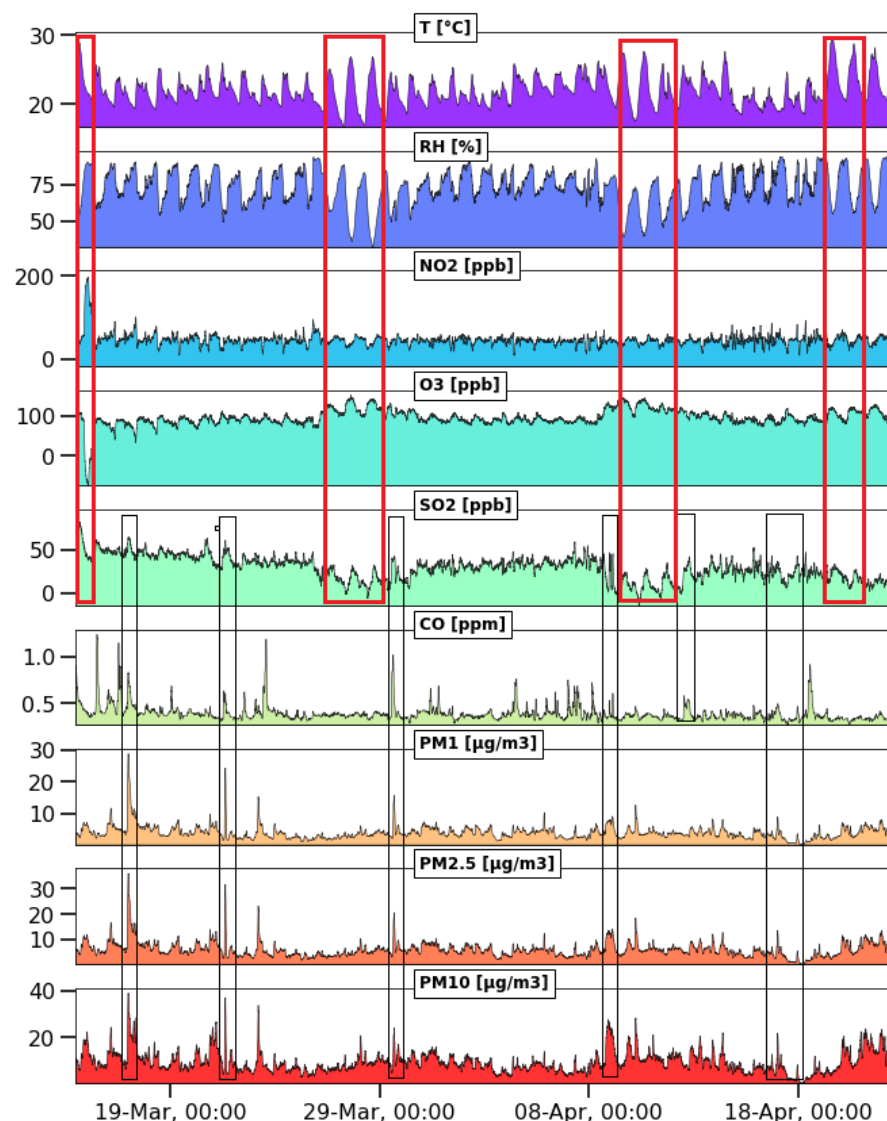


Figure 7. Results of the measuring campaign at Cienfuegos, Cuba with the low-cost monitoring system from 14 March to 22 April 2022. The red rectangles indicate the simultaneous relationship of SO_2 with some parameters such as temperature, relative humidity, NO_2 and O_3 . The black rectangles indicate the simultaneous relationship of SO_2 with CO and particulate matter. All parameters have been recorded by low-cost sensors.

Figure 8 shows the correlation coefficients between the variables recorded by the low-cost monitoring system used in Cienfuegos, Cuba. The numbers vary between -1 and 1 , indicating the linear relationship between two variables and, in this case, between the measured pollutants. The linear correlation of SO_2 with the rest of the variables takes values close to zero, resulting in a low correlation. The most influential pollutant was O_3 , followed by CO with a correlation coefficient of -0.5 and 0.45 , respectively, which might be caused by interference and be corrected with the equations in Figure 4b. This means that during the measuring campaign, the SO_2 sensor was not strongly influenced by the other pollutants and neither by temperature nor relative humidity.

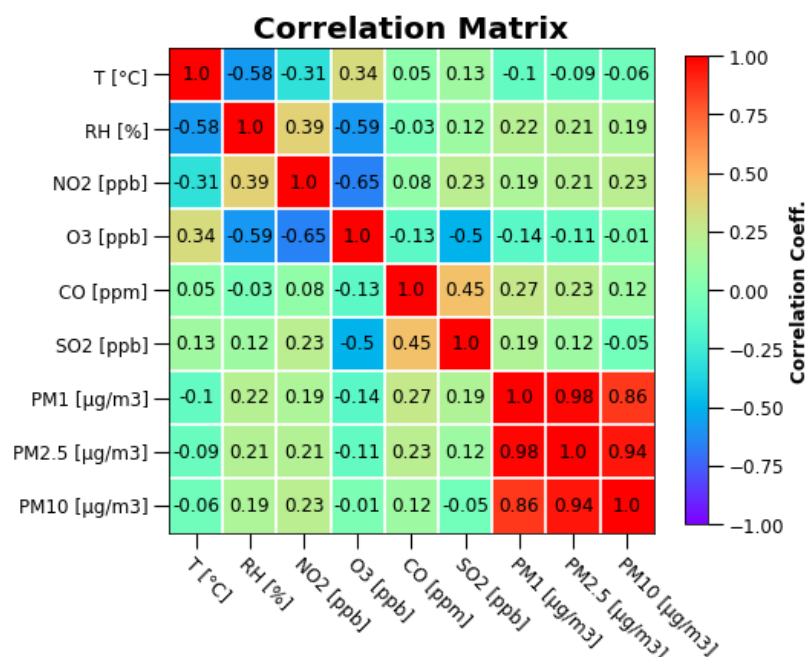


Figure 8. Correlation matrix between the different pollutants and meteorological variables recorded during the measuring campaign at Cienfuegos, Cuba.

5. Conclusions

Many publications assess the quality of low-cost sensors by comparing their measurements to those obtained from state-of-the-art reference instruments. In this study, the evaluation of low-cost sensors encompasses a broader range of indicators. While the accuracy and precision of the low-cost sensor in relation to advanced reference instruments are considered in the assessment, the focus is primarily on the extent of meaningful information that can be derived from low-cost sensors. This approach offers a significant advantage, as it enables the utilization of low-cost sensors in addressing pollution-related issues, even if they are not as accurate as state-of-the-art reference instruments.

Several indicators allowed us to analyse the reliability of the SO₂ Alphasense gas sensor. This sensor did not result in reliable results during the field calibration in Belgium because, in the city of Antwerp, the background concentrations in ambient air were too low. However, the same sensor resulted in reliable data in Cuba due to higher background concentrations. In addition, the SO₂ gas sensor could be calibrated using low-cost equipment in a tropical climate, showing a strong linear relationship with the reference concentrations. This means that low- and middle-income countries are able to calibrate the SO₂ sensor with a restricted budget. Calibration methods performed with different methods at different moments and on different continents can be compared with each other when the background baseline $WE_{background}$ can be subtracted from the signal in an accurate way. The reliability of the sensor is limited by the cross-sensitivity effect, with O₃ being the most interfering gas in the SO₂ sensor. In addition, the sensor signal appears to be more reliable when ambient conditions are below 30 °C and above 40% relative humidity. By showing the reliability of low-cost gas sensors, such as the SO₂ sensor used in this study, numerous institutions and researchers from low- and middle-income countries gain access to research infrastructure to solve local problems. This makes scientific research more inclusive.

The mathematical derivations given in this contribution show that the background level $WE_{background}$ can be calculated when WE_0 and AE_0 are known. However, the values for WE_0 and AE_0 obtained by zero calibration were strongly affected by the sampling location. Moreover, $WE_{background}$ also appeared to evolve in a fixed location over time. To improve the conversion method of sensor signals into concentration, more research is needed to understand how WE_0 and AE_0 are affected by the measuring location and

the meteorological conditions and how stable they are at a fixed location. For this, more experiments in zero air are needed. The study also suggests that the span calibration is more stable in relation to location and time than the zero calibration, but this suggestion needs to be investigated in more detail by performing consecutive calibrations over time. Finally, one can wonder how in situ calibration can be done to improve sensor reliability.

Author Contributions: R.A.G.R.: Data processing and analysis of results obtained in the SO₂ sensor calibration and manuscript preparation. O.S.: Research conception and design; preparation, review, and approval of the final version of the manuscript. A.A.C.: Data processing of the results obtained in the field campaigns. E.H.R.: Design of the low-cost monitoring system. M.C.M.P.: Sampling site selection strategy and processing of the data obtained in the field campaigns. D.A.S.: Research conception and design; review and approval of the final version of the manuscript. A.M.L.: Assembly of the low-cost monitoring system; review and approval of the final version of the manuscript. W.J.: Research conception and design; review and approval of the final version of the manuscript. L.H.S.: Research conception and design; review and approval of the final version of the manuscript. All authors have read and agreed to the published version of the manuscript.

Funding: The present work has been supported by the VLIR-UOS Program as a South Initiative Project SI-2019 nr. CU2019SIN242B124 “AIR@PORT: Low-cost decision support system to evaluate the impact of ships on the air quality in the port city Cienfuegos”. Additional financial support has been given by the Common Global Minds Project BE2017GMHVLHC106 of all Flemish Universities of Applied Sciences and Arts.

Institutional Review Board Statement: Not applicable.

Informed Consent Statement: Not applicable.

Data Availability Statement: All data used in this study are available upon request.

Acknowledgments: The authors thank VLIR-UOS for their financial support of the South Initiative Project SI-2019 nr. CU2019SIN242B124 “AIR@PORT: Low-cost decision support system to evaluate the impact of ships on the air quality in the port city Cienfuegos”. They are also grateful for the additional support provided by the Global Minds project BE2017GMHVLHC106 “A low-cost measuring device to directly monitor exhaust gases generated by fuel engines: Design, development, validation”. The researchers are grateful to the VMM for allowing them to measure near one of their monitoring stations.

Conflicts of Interest: The authors declare no conflict of interest.

References

1. Rosen, C.M. Businessmen Against Pollution in Late Nineteenth Century Chicago. *Bus. Hist. Rev.* **1995**, *69*, 351–397. [[CrossRef](#)]
2. Wisniak, J. Sodium Carbonate—From Natural Resources to Leblanc and Back. *Indian J. Chem. Technol.* **2003**, *10*, 99–112.
3. Dingle, A.E. ‘The Monster Nuisance of All’: Landowners, Alkali Manufacturers, and Air Pollution, 1828–64. *Econ. Hist. Rev.* **1982**, *35*, 529–548. [[CrossRef](#)]
4. Nemery, B.; Hoet, P.H.; Nemmar, A. The Meuse Valley Fog of 1930: An Air Pollution Disaster. *Lancet* **2001**, *357*, 704–708. [[CrossRef](#)]
5. Firket, J. Fog along the Meuse Valley. *Trans. Faraday Soc.* **1936**, *32*, 1192. [[CrossRef](#)]
6. Medlin, J. Toxicogenomics Research Consortium Sails into Uncharted Waters. *Environ. Health Perspect.* **2002**, *110*, A744–A746. [[CrossRef](#)] [[PubMed](#)]
7. Scott, J.A. Fog and Deaths in London, December 1952. *Public Health Rep.* **1953**, *68*, 474. [[CrossRef](#)]
8. Schwartz, J.; Marcus, A. Mortality and Air Pollution in London: A Time Series Analysis. *Am. J. Epidemiol.* **1990**, *131*, 185–194. [[CrossRef](#)]
9. Bell, M.L.; Davis, D.L. Reassessment of the Lethal London Fog of 1952: Novel Indicators of Acute and Chronic Consequences of Acute Exposure to Air Pollution. *Environ. Health Perspect.* **2001**, *109*, 389–394.
10. Stern, A.C.; Professor, E. History of Air Pollution Legislation in the United States. *J. Air Pollut. Control Assoc.* **1982**, *32*, 44–61. [[CrossRef](#)]
11. Valler, R.E.; Lawther, P.J. Further Observation of London Fog. *BMJ* **1957**, *2*, 1473–1475. [[CrossRef](#)]
12. Mylona, S. Sulphur Dioxide Emissions in Europe 1880–1991 and Their Effect on Sulphur Concentrations and Depositions. *Tellus B* **1996**, *48*, 662–689. [[CrossRef](#)]
13. Fowler, D.; Brimblecombe, P.; Burrows, J.; Heal, M.R.; Grennfelt, P.; Stevenson, D.S.; Jowett, A.; Nemitz, E.; Coyle, M.; Liu, X.; et al. A Chronology of Global Air Quality. *Phil. Trans. R. Soc. A.* **2020**, *378*, 20190314. [[CrossRef](#)] [[PubMed](#)]

14. Van Roy, W.; Van Nieuwenhove, A.; Scheldeman, K.; Van Roozendaal, B.; Schallier, R.; Mellqvist, J.; Maes, F. Measurement of Sulfur-Dioxide Emissions from Ocean-Going Vessels in Belgium Using Novel Techniques. *Atmosphere* **2022**, *13*, 1756. [CrossRef]
15. Krupińska, B.; Worobiec, A.; Gatto Rotondo, G.; Novaković, V.; Kontozova, V.; Ro, C.-U.; Van Grieken, R.; De Wael, K. Assessment of the Air Quality (NO₂, SO₂, O₃ and Particulate Matter) in the Plantin-Moretus Museum/Print Room in Antwerp, Belgium, in Different Seasons of the Year. *Microchem. J.* **2012**, *102*, 49–53. [CrossRef]
16. Henschel, S.; Querol, X.; Atkinson, R.; Pandolfi, M.; Zeka, A.; Le Tertre, A.; Analitis, A.; Katsouyanni, K.; Chanel, O.; Pascal, M.; et al. Ambient Air SO₂ Patterns in 6 European Cities. *Atmos. Environ.* **2013**, *79*, 236–247. [CrossRef]
17. Magaña, M.; Sánchez, C. Efectos del petróleo crudo cubano sobre los procesos de lixiviación, sedimentación y destilación en Nicaro. *RTQ* **2015**, *35*, 54–62.
18. Veloz, L.A.; Sandoval, F.D. *Caracterización Físico-Química de Crudos Cubanos de las Estructuras en Evaluación del Bloque VIIA de la Franja Norte de Crudos Pesados*; Pueblo y Educación: La Habana, Cuba, 2011; pp. 1–9.
19. Hernández, A.R.; Quintero, J.O.L.; Clemente, A.N.; Cano, C.; Lopez, O.D. Caracterización de la fracción saturada de petróleos del yacimiento Varadero, mediante cromatografía gaseosa. *Rev. CENIC Cienc. Quím.* **2021**, *52*, 81–91.
20. EnerTechUp GmbH. Advanced Energy Technology. Available online: <https://aenert.com/countries/america/energy-industry-in-cuba/general-data/> (accessed on 10 February 2023).
21. Cuesta-Santos, O.; Sosa-Pérez, C.; Iraola-Ramírez, C.; González, Y.; Nuñez-Caraballo, V.; Fonte-Hernández, A.; Imbert-Lamorú, C.; Gómez-Zamora, Y.; Portal-Castillo, D. Inventario nacional de emisiones atmosféricas de las principales fuentes fijas. *Rev. Cuba. Meteorol.* **2017**, *23*, 178–190.
22. Cruz-Montes de Oca, F.; Furet-Bridón, N.R.; Turtós-Carbonell, L.; Lorente-Vera, M. La dispersión atmosférica de contaminantes en una zona industrial de Cuba. *Rev. CENIC Cienc. Quím.* **2011**, *42*, 1–7.
23. Alejo, D.; Morales, M.C.; De la Torre, J.B.; Grau, R.; Bencs, L.; Grieken, R.V.; Espen, P.V.; Sosa, D.; Nuñez, V. Seasonal Trends of Atmospheric Nitrogen Dioxide and Sulfur Dioxide over North Santa Clara, Cuba. *Environ. Monit. Assess.* **2013**, *185*, 6023–6033. [CrossRef] [PubMed]
24. Madrazo, J.; Clappier, A.; Cuesta, O.; Belalcazar, L.C.; González, Y.; Bolufé, J.; Sosa, C.; Carrillo, E.; Manso, R.; Canciano, J.; et al. Evidence of Traffic-Generated Air Pollution in Havana. *Atmosfera* **2019**, *32*, 15–24. [CrossRef]
25. Schalm, O.; Carro, G.; Lazarov, B.; Jacobs, W.; Stranger, M. Reliability of Lower-Cost Sensors in the Analysis of Indoor Air Quality on Board Ships. *Atmosphere* **2022**, *13*, 1579. [CrossRef]
26. Narayana, M.V.; Jalihal, D.; Nagendra, S.M.S. Establishing A Sustainable Low-Cost Air Quality Monitoring Setup: A Survey of the State-of-the-Art. *Sensors* **2022**, *22*, 394. [CrossRef]
27. Hagan, D.H.; Isaacman-VanWertz, G.; Franklin, J.P.; Wallace, L.M.M.; Kocar, B.D.; Heald, C.L.; Kroll, J.H. Calibration and Assessment of Electrochemical Air Quality Sensors by Co-Location with Regulatory-Grade Instruments. *Atmos. Meas. Tech.* **2018**, *11*, 315–328. [CrossRef]
28. Drajić, D.D.; Gligorić, N.R. Reliable Low-Cost Air Quality Monitoring Using Off-The-Shelf Sensors and Statistical Calibration. *Elektron. Elektrotech.* **2020**, *26*, 32–41. [CrossRef]
29. Chojer, H.; Branco, P.T.B.S.; Martins, F.G.; Alvim-Ferraz, M.C.M.; Sousa, S.I.V. Can Data Reliability of Low-Cost Sensor Devices for Indoor Air Particulate Matter Monitoring Be Improved?—An Approach Using Machine Learning. *Atmos. Environ.* **2022**, *286*, 119251. [CrossRef]
30. Doval-Miñarro, M.; Bueso, M.C. A Comparative Study of Air Pollutant Concentrations before the COVID-19 Pandemic and in the New Normal in the Región de Murcia (Spain). *Atmosphere* **2023**, *14*, 147. [CrossRef]
31. Dimov, I.; Todorov, V.; Sabelfeld, K. A Study of Highly Efficient Stochastic Sequences for Multidimensional Sensitivity Analysis. *Monte Carlo Methods Appl.* **2022**, *8*, 1–12. [CrossRef]
32. Rhouati, A.; Berkani, M.; Vasseghian, Y.; Golzadeh, N. MXene-Based Electrochemical Sensors for Detection of Environmental Pollutants: A Comprehensive Review. *Chemosphere* **2022**, *291*, 132921. [CrossRef]
33. Farquhar, A.K.; Henshaw, G.S.; Williams, D.E. Errors in Ambient Gas Concentration Measurement Caused by Acoustic Response of Electrochemical Gas Sensors. *Sens. Actuator A Phys.* **2023**, *354*, 114254. [CrossRef]
34. Williams, D.E. Electrochemical Sensors for Environmental Gas Analysis. *Curr. Opin. Electrochem.* **2020**, *22*, 145–153. [CrossRef]
35. Silambarasan, P.; Moon, I.S. Real-Time Monitoring of Chlorobenzene Gas Using an Electrochemical Gas Sensor during Mediated Electrochemical Degradation at Room Temperature. *J. Electroanal. Chem.* **2021**, *894*, 115372. [CrossRef]
36. Todorov, V.; Ostromsky, T.; Dimov, I.; Fidanova, S. Optimized Quasi-Monte Carlo Method Based on Low Discrepancy Sequences for Sensitivity Analysis in Air Pollution Modelling. 26 September 2020. pp. 25–28. Available online: https://www.researchgate.net/publication/346122855_Optimized_Quasi-Monte_Carlo_Method_Based_on_Low_Discrepancy_Sequences_for_Sensitivity_Analysis_in_Air_Pollution_Modelling (accessed on 1 March 2023).
37. Soares, P.H.; Monteiro, J.P.; Gaioto, F.J.; Ogiboski, L.; Andrade, C.M.G. Use of Association Algorithms in Air Quality Monitoring. *Atmosphere* **2023**, *14*, 648. [CrossRef]
38. Samad, A.; Obando Nuñez, D.R.; Solís Castillo, G.C.; Laquai, B.; Vogt, U. Effect of Relative Humidity and Air Temperature on the Results Obtained from Low-Cost Gas Sensors for Ambient Air Quality Measurements. *Sensors* **2020**, *20*, 5175. [CrossRef]
39. Masic, A.; Bibic, D.; Pikula, B.; Razic, F. New Approach of Measuring Toxic Gases Concentrations: Principle of Operation. In *DAAAM Proceedings*; Katalinic, B., Ed.; DAAAM International Vienna: Vienna, Austria, 2018; Volume 1, pp. 0882–0887, ISBN 978-3-902734-20-4.

40. Zuidema, C.; Schumacher, C.S.; Austin, E.; Carvlin, G.; Larson, T.V.; Spalt, E.W.; Zusman, M.; Gasset, A.J.; Seto, E.; Kaufman, J.D.; et al. Deployment, Calibration, and Cross-Validation of Low-Cost Electrochemical Sensors for Carbon Monoxide, Nitrogen Oxides, and Ozone for an Epidemiological Study. *Sensors* **2021**, *21*, 4214. [[CrossRef](#)]
41. Tryner, J.; Phillips, M.; Quinn, C.; Neymark, G.; Wilson, A.; Jathar, S.H.; Carter, E.; Volckens, J. Design and Testing of a Low-Cost Sensor and Sampling Platform for Indoor Air Quality. *Buill. Environ.* **2021**, *206*, 108398. [[CrossRef](#)]
42. Arroyo, P.; Gómez-Suárez, J.; Suárez, J.I.; Lozano, J. Low-Cost Air Quality Measurement System Based on Electrochemical and PM Sensors with Cloud Connection. *Sensors* **2021**, *21*, 6228. [[CrossRef](#)]
43. Sensor Technology House. *Alphasense Application Note AAN 803-04 Correcting for Background Currents in Four Electrode Toxic Gas Sensors*; Alphasense Limited: Heywood, UK, 2017.
44. Alphasense Application Notes. Available online: www.alphasense.com (accessed on 20 March 2023).
45. Cross, E.S.; Lewis, D.K.; Williams, L.R.; Magoon, G.R.; Kaminsky, M.L.; Worsnop, D.R.; Jayne, J.T. Use of Electrochemical Sensors for Measurement of Air Pollution: Correcting Interference Response and Validating Measurements. *Atmos. Meas. Tech.* **2017**, *10*. [[CrossRef](#)]
46. Hernandez-Rodriguez, E.; Kairuz-Cabrera, D.; Martinez, A.; Amalia, R.; Schalm, O. Low-Cost Portable System for the Estimation of Air Quality. In *Proceedings of 19th Latin American Control Congress (LACC 2022)*; Studies in Systems, Decision and Control; Springer: La Habana, Cuba, 2022; Volume 464, p. XII, ISBN 978-3-031-26361-3.
47. Martinez, A.; Hernandez-Rodriguez, E.; Hernandez, L.; González-Rivero, R.A.; Alejo-Sánchez, D.; Schalm, O. Design of a Low-Cost Portable System for the Measurement of Variables Associated with Air Quality. *IEEE Embed. Syst.* **2022**. [[CrossRef](#)]
48. Margaritis, D.; Keramydas, C.; Papachristos, I.; Lambropoulou, D. Calibration of Low-Cost Gas Sensors for Air Quality Monitoring. *Aerosol Air Qual. Res.* **2021**, *21*, 210073. [[CrossRef](#)]
49. Maag, B.; Zhou, Z.; Thiele, L. A Survey on Sensor Calibration in Air Pollution Monitoring Deployments. *IEEE Internet Things J.* **2018**, *5*, 4857–4870. [[CrossRef](#)]
50. Spinelle, L.; Aleixandre, M.; Gerboles, M. *Protocol of Evaluation and Calibration of Low-Cost Gas Sensors for the Monitoring of Air Pollution*; Publication Office of the European Union: Luxembourg, 2013.
51. Mijling, B.; Jiang, Q.; de Jonge, D.; Bocconi, S. Field Calibration of Electrochemical NO₂ Sensors in a Citizen Science Context. *Atmos. Meas. Tech.* **2018**, *11*, 1297–1312. [[CrossRef](#)]
52. Topalović, D.B.; Davidović, M.D.; Jovanović, M.; Bartonova, A.; Ristovski, Z.; Jovašević-Stojanović, M. In Search of an Optimal In-Field Calibration Method of Low-Cost Gas Sensors for Ambient Air Pollutants: Comparison of Linear, Multilinear and Artificial Neural Network Approaches. *Atmos. Environ.* **2019**, *213*, 640–658. [[CrossRef](#)]
53. González Rivero, R.A.; Morera Hernández, L.E.; Schalm, O.; Hernández Rodríguez, E.; Alejo Sánchez, D.; Morales Pérez, M.C.; Nuñez Caraballo, V.; Jacobs, W.; Martínez Laguardia, A. A Low-Cost Calibration Method for Temperature, Relative Humidity, and Carbon Dioxide Sensors Used in Air Quality Monitoring Systems. *Atmosphere* **2023**, *14*, 191. [[CrossRef](#)]
54. Mattson, B. Microscale Gas Chemistry. *Educ. Quim.* **2018**, *16*, 514. [[CrossRef](#)]
55. Najdoski, M. Gas Chemistry: A Microscale Kipp Apparatus. *J. Chem. Educ.* **2011**, *16*, 295–298.
56. Najdoski, M.; Stojković, S. Cost Effective Microscale Gas Generation Apparatus. *Chemistry* **2010**, *19*, 444–449.
57. Zimmerman, N.; Presto, A.A.; Kumar, S.P.N.; Gu, J.; Haurlyuk, A.; Robinson, E.S.; Robinson, A.L.; Subramanian, R. Closing the Gap on Lower Cost Air Quality Monitoring: Machine Learning Calibration Models to Improve Low-Cost Sensor Performance. *Atmos. Meas. Tech.* **2017**. [[CrossRef](#)]
58. Carro, G.; Schalm, O.; Jacobs, W.; Demeyer, S. Exploring Actionable Visualizations for Environmental Data: Air Quality Assessment of Two Belgian Locations. *Environ. Model. Softw.* **2022**, *147*, 105230. [[CrossRef](#)]
59. Lewis, A.C.; Lee, J.D.; Edwards, P.M.; Shaw, M.D.; Evans, M.J.; Moller, S.J.; Smith, K.R.; Buckley, J.W.; Ellis, M.; Gillot, S.R.; et al. Evaluating the Performance of Low Cost Chemical Sensors for Air Pollution Research. *Faraday Discuss.* **2016**, *189*, 85–103. [[CrossRef](#)] [[PubMed](#)]
60. Gamboa, V.S.; Kinast, É.J.; Pires, M. System for Performance Evaluation and Calibration of Low-Cost Gas Sensors Applied to Air Quality Monitoring. *Atmos. Pollut. Res.* **2023**, *14*, 101645. [[CrossRef](#)]
61. Pang, X.; Shaw, M.D.; Gillot, S.; Lewis, A.C. The Impacts of Water Vapour and Co-Pollutants on the Performance of Electrochemical Gas Sensors Used for Air Quality Monitoring. *Sens. Actuators B Chem.* **2018**, *266*, 674–684. [[CrossRef](#)]
62. Wei, P.; Ning, Z.; Ye, S.; Sun, L.; Yang, F.; Wong, K.; Westerdahl, D.; Louie, P. Impact Analysis of Temperature and Humidity Conditions on Electrochemical Sensor Response in Ambient Air Quality Monitoring. *Sensors* **2018**, *18*, 59. [[CrossRef](#)] [[PubMed](#)]
63. NC 111: 2004; Calidad del Aire—Reglas para la Vigilancia de la Calidad del Aire en Asentamientos Humanos. Cuban National Bureau of Standards: La Habana, Cuba, 2004.
64. Langford, G.O.; Winefordner, J.D. Limit of Detection. A Closer Look at the IUPAC Definition. *Anal. Chem.* **1983**, *55*, 712–724. [[CrossRef](#)]
65. Alejo, D.; Morales, M.C.; Nuñez, V.; Bencs, L.; Van Grieken, R.; Van Espen, P. Monitoring of Tropospheric Ozone in the Ambient Air with Passive Samplers. *Microchem. J.* **2011**, *99*, 383–387. [[CrossRef](#)]
66. NC 39:1999; Calidad Del Aire. Requisitos Higiénicos—Sanitarios. Cuban National Bureau of Standards: La Habana, Cuba, 1999.
67. Cui, H.; Zhang, L.; Li, W.; Yuan, Z.; Wu, M.; Wang, C.; Ma, J.; Li, Y. A New Calibration System for Low-Cost Sensor Network in Air Pollution Monitoring. *Atmos. Pollut. Res.* **2021**, *12*, 101049. [[CrossRef](#)]

68. Schalm, O.; Carro, G.; Jacobs, W.; Lazarov, B.; Stranger, M. The Inherent Instability of Environmental Parameters Governing Indoor Air Quality on Board Ships and the Use of Temporal Trends to Identify Pollution Sources. *Indoor Air* **2023**, *2023*, 1–19. [[CrossRef](#)]
69. Wenzel, M.J.; Mensah-Brown, A.; Josse, F.; Yaz, E.E. Online Drift Compensation for Chemical Sensors Using Estimation Theory. *IEEE Sens. J.* **2011**, *11*, 225–232. [[CrossRef](#)]
70. Instituto de Meteorología de Cuba. Available online: <http://www.insmet.cu> (accessed on 7 May 2023).
71. Stewart, G.J.; Acton, W.J.F.; Nelson, B.S.; Vaughan, A.R.; Hopkins, J.R.; Arya, R.; Mondal, A.; Jangirh, R.; Ahlawat, S.; Yadav, L.; et al. Emissions of Non-Methane Volatile Organic Compounds from Combustion of Domestic Fuels in Delhi, India. *Atmos. Chem. Phys.* **2021**, *21*, 2383–2406. [[CrossRef](#)]
72. İlkiliç, C.; Aydin, H. The Harmful Effects of Diesel Engine Exhaust Emissions. *Energy Sources Part A Recovery Util. Environ. Eff.* **2012**, *34*, 899–905. [[CrossRef](#)]
73. Cofer, W.R.; Schryer, D.R.; Rogowski, R.S. Oxidation of SO₂ by NO₂ and O₃ on Carbon: Implications to Tropospheric Chemistry. *Atmos. Environ.* **1984**, *18*, 243–245. [[CrossRef](#)]

Disclaimer/Publisher's Note: The statements, opinions and data contained in all publications are solely those of the individual author(s) and contributor(s) and not of MDPI and/or the editor(s). MDPI and/or the editor(s) disclaim responsibility for any injury to people or property resulting from any ideas, methods, instructions or products referred to in the content.